PHYSICAL REVIEW B **76**, 060404(R) (2007)

Colossal magnon-phonon coupling in multiferroic $Eu_{0.75}Y_{0.25}MnO_3$

R. Valdés Aguilar,[1] A. B. Sushkov,[1] C. L. Zhang,[2] Y. J. Choi,[2] S.-W. Cheong,[2] and H. D. Drew[1]
[1]*Materials Research Science and Engineering Center, University of Maryland, College Park, Maryland 20742, USA*
[2]*Rutgers Center for Emergent Materials and Department of Physics & Astronomy, Rutgers University, Piscataway, New Jersey 08854, USA*

(Received 20 June 2007; published 15 August 2007)

We report the spectra of magnetically induced electric dipole absorption in $Eu_{0.75}Y_{0.25}MnO_3$ from temperature-dependent far-infrared spectroscopy (10–250 cm^{-1}). These spectra, which occur only in the $e\|a$ polarization, consist of two relatively narrow electromagnon features with onset at $T_{FE}=30$ K and a broad absorption band that persists to temperatures well above $T_N=47$ K. The observed excitations account for the step up of the static dielectric constant in the ferroelectric phase. The electromagnon at 80 cm^{-1} is observed to be strongly coupled to the nearby lowest optical phonon which transfers more than 1/2 of its spectral weight to the magnon. We attribute the origin of the broad background absorption to the two-magnon-emission decay process of the phonon.

DOI: 10.1103/PhysRevB.76.060404 PACS number(s): 75.80.+q, 63.20.Ls, 75.30.Et, 76.50.+g

In multiferroic materials the simultaneous magnetic and ferroelectric order can produce cross coupling between electric and magnetic signals.[1] This prospect has important implications for electronic memory and logic applications. On the other hand, multiferroics exhibit interesting new fundamental features. The absence of both time and space inversion symmetry in relatively low-symmetry crystal structures can produce a rich array of novel magnetoelectric phenomena. One such effect is the coupling between the low-lying magnetic and lattice excitations to produce spin waves that interact strongly with light by acquiring electric dipole activity from the phonons.[2,3] These excitations, called electromagnons,[4,5] can thereby produce contributions to the static dielectric constant which appear in the ordered phases and that can be manipulated with an applied magnetic field. This may be the origin of the giant magnetocapacitance effect observed in these materials.[6,7] The magnitude of this effect is related to the strength of the coupling between the optically active phonons and the low-lying spin waves. Therefore, further enhancement of the effect may be achieved in materials that favor a strong magnon-phonon coupling.

Few multiferroic systems with strong magnetoelectric effects are known since proper ferroelectricity and magnetism are usually antithetic.[8] Much of the current interest is in multiferroicity with improper ferroelectricity, which is induced by exchange striction in magnetically ordered states with broken spatial inversion symmetry.[1] This produces strongly coupled multiferroics. They are found in materials with frustrated magnetic exchange and noncollinear spin order. One example is the family of compounds $RMnO_3$ (R =Tb,Dy,Gd,Eu–Y), whose static properties have been studied extensively.[7,9] In $TbMnO_3$,[10] for example, the appearance of ferroelectricity coincides with the transition of the Mn spin system into an antiferromagnetic structure with spiral order.

The understanding of the origin of the magnetically induced improper ferroelectricity is still evolving. The broken inversion symmetry of the magnetic structure is only a necessary condition for the existence of spontaneous polarization[11,12] and cannot be used to uniquely identify the coupling mechanism. The presence of competing exchange processes produces the ferroelectric order but complicates the understanding. Therefore we have studied the dynamical response, which provides additional symmetry information through the optical selection rules and gives insight into the low-lying magnetic and lattice excitations.

Pimenov *et al.*[4,13] reported the observation of an electric dipole active magnon, an electromagnon, in the low-energy electrodynamic response of Tb and $GdMnO_3$. However, this identification was not conclusive as Tb has partially filled f shells with low-lying levels that can also give rise to electric dipole excitations in this frequency range.[14] A positive identification of the electromagnon has been made in the related multiferroic compound YMn_2O_5.[5] Since the f shell in Y^{3+} ion is completely empty, the observed excitations arise entirely from the Mn spin system.

However, the $RMnO_3$ system is attractive because it has simpler crystalline and magnetic order, which may facilitate the unraveling of the complex physics of multiferroicity. Moreover, in addition to the ambiguity due to f levels, the accuracy of the infrared (ir) data in the original reports on Tb and $GdMnO_3$ was limited. In this Rapid Communication we report ir measurements on $Eu_{1-x}Y_xMnO_3$ in which Mn^{3+} is the only magnetic ion. We have chosen $Eu_{0.75}Y_{0.25}MnO_3$ because it is close in structural, magnetic, and multiferroic properties to $TbMnO_3$. In addition to observing electromagnons in this compound without low-energy f levels, which affirms the existence of electromagnons in the orthorhombic $RMnO_3$ system, we also report a strikingly strong coupling between magnons and phonons in $Eu_{0.75}Y_{0.25}MnO_3$, in which more than 1/2 of the dipole oscillator strength of a phonon is transferred to a spin excitation.

Single crystals of $Eu_{0.75}Y_{0.25}MnO_3$ were grown as described elsewhere.[15] The samples were characterized by x-ray diffraction and dielectric measurements in the kilohertz range. Our samples are ferroelectric below $T_{FE}=30$ K with static polarization in the a-c plane ($\mathbf{P}_a \gg \mathbf{P}_c$), and magnetically ordered with transition temperature $T_N=47$ K; the magnetic structure is still unknown. Optical measurements of re-

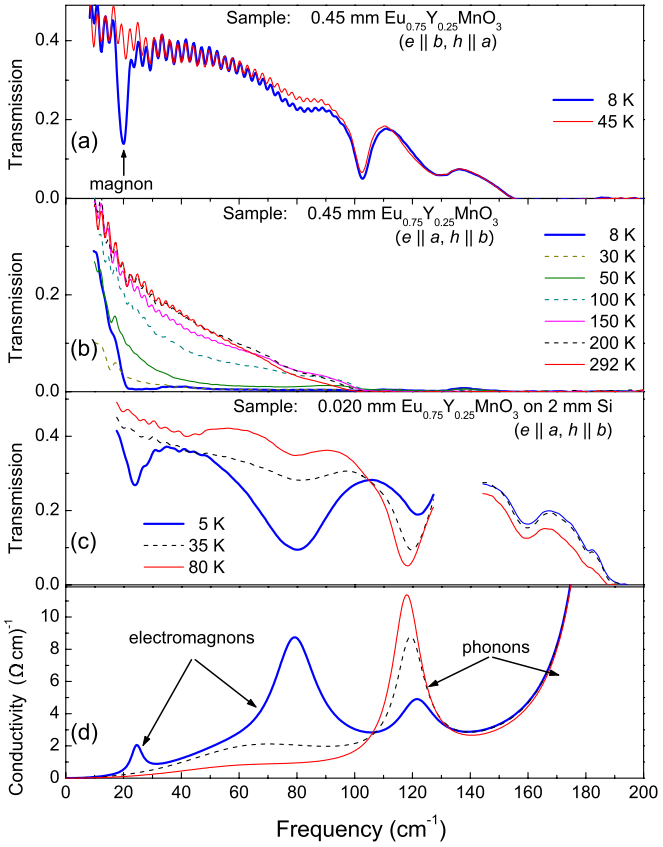

FIG. 1. (Color online) (a), (b), (c) Transmission spectra of $Eu_{0.75}Y_{0.25}MnO_3$ in different polarization configurations; (d) optical conductivity from fits of spectra in (c). e and h are electric and magnetic fields of light.

flectance and transmission were made as a function of temperature as described elsewhere.[5] The transmission of an a-b plane crystal was measured at thicknesses of 1.93, 0.45, 0.080, and 0.020 mm. A second crystal was measured in a-c plane geometry at 1.28 mm thickness.

To extract the temperature dependence of the optical conductivity we fit the transmission spectra with a Lorentzian model of the dielectric constant $\varepsilon(\omega)$ for electric dipole and/or magnetic permeability $\mu(\omega)$ for magnetic dipole transitions as described elsewhere:[5,15]

$$\varepsilon(\omega) = \varepsilon_\infty + \sum_j \frac{S_j}{\omega_j^2 - \omega^2 - \imath\omega\gamma_j}, \quad (1)$$

$$\mu(\omega) = 1 + \sum_k \frac{M_k}{\omega_k^2 - \omega^2 - \imath\omega\gamma_k}, \quad (2)$$

where ε_∞ is the high-frequency dielectric constant, j,k enumerate the oscillators, S_j and M_k are spectral weights, $\omega_{j,k}$ is the resonance frequency, and $\gamma_{j,k}$ is the damping rate.

The striking difference between Figs. 1(a) and 1(b) corresponds to the magnetic dipole and electric dipole absorptions at low temperature for the same thickness. The transmission spectra show that a strong low-frequency absorption in $Eu_{0.75}Y_{0.25}MnO_3$ occurs only in $e\|a$ polarization—as was

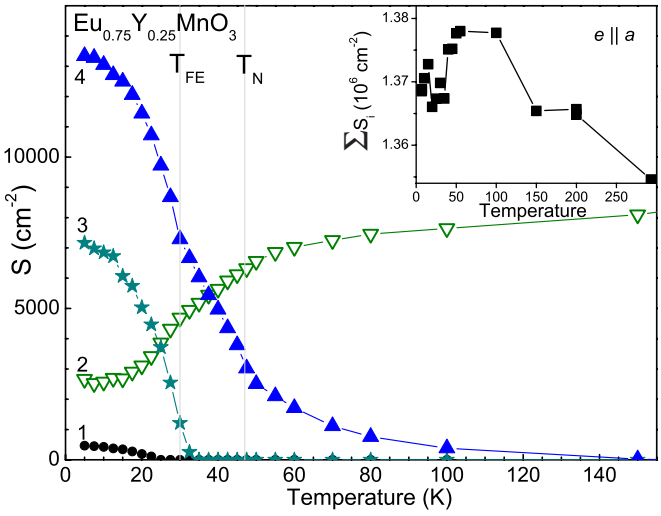

FIG. 2. (Color online) Spectral weight of the features below 140 cm^{-1}. Curves show data for (1) 25 cm^{-1} peak, (2) 120 cm^{-1} phonon, (3) peak at ~80 cm^{-1}, and (4) total spectral weight below 140 cm^{-1} (excluding the phonon). Inset: Total spectral weight of the eight phonons above 140 cm^{-1}.

reported for $TbMnO_3$ and $GdMnO_3$.[4] In $e\|c$, the ir-active phonons are the only electric dipole features observed (not shown). In the $(e\|b, h\|a)$ polarization we found only one weak absorption mode below T_N [Fig. 1(a)]. Fitting this mode as an $h\|a$ magnetic-dipole-active antiferromagnetic resonance (AFMR) gives the values $\omega = 20$ cm^{-1}, $\gamma = 2.3$ cm^{-1}, and $M = 2.5$ cm^{-2} at 8 K which are typical for AFMR.[5] In this fit we used $\varepsilon = 17.5$, which was obtained by fitting $e\|b$ phonon reflectivity spectra. This resonance was also observed in the $e\|c$, $h\|a$ configuration on the a-c plane sample (not shown).

We used a much thinner sample to quantify the $e\|a$ spectra as shown in Fig. 1(c). Below T_{FE}, two relatively narrow features appear: a low-energy peak at 25 cm^{-1} and a broader absorption at 80 cm^{-1}. The gap in the Fig. 1(c) data near 140 cm^{-1} is due to absorption in the cold quartz window. An isosbestic point (frequency of constant absorption) is found at 105 cm^{-1} which signifies spectral weight conservation between the low-frequency absorption and the phonons. We have observed similar features at 25 and 65 cm^{-1} in a polycrystal of $TbMnO_3$.

A broad background in absorption is observed [Fig. 1(b)] in $e\|a$ (but not in the $e\|b$ or $e\|c$ polarizations) and persists to temperatures as high as 150 K. In Fig. 2 we show that this background absorption grows in strength as T decreases (filled upright triangles) and this growth accelerates below $T = T_N$. At $T = 10$ K the background accounts for approximately half of the total low-frequency oscillator strength below 140 cm^{-1}.

The optical conductivity obtained by fitting the transmission spectra of Fig. 1(c) is shown in Fig. 1(d). We used three Lorentzians to fit the spectra. Their parameters are (ω, γ, S) at 5 K (25, 4, 467), (65, 70, 7708), (79, 17, 7506). The spectral weight of the lowest-frequency peak is comparable to the corresponding values for the electromagnons in YMn_2O_5 and $TbMn_2O_5$.[5] The phonon parameters are (122, 15, 2662) at 5 K and (118, 12, 7456) at 80 K.

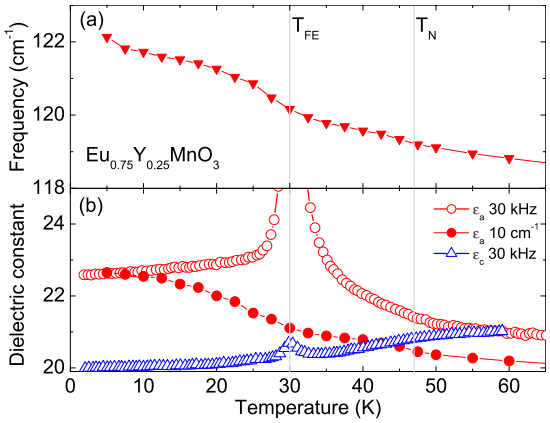

FIG. 3. (Color online) (a) Temperature dependence of the phonon frequency that shows hardening at T_{FE}. (b) Dielectric constant of $Eu_{0.75}Y_{0.25}MnO_3$ from fits of infrared spectra in comparison with 30 kHz measurements.

The frequencies of the 25 and 80 cm^{-1} peaks show very little temperature dependence and the damping rate decreases, both below T_{FE} (not shown). The temperature dependence of the spectral weight of the low-frequency modes is shown in Fig. 2. We note that the phonon spectral weight begins changing significantly around T_N and shows an inflection point at T_{FE}, signaling coupling to the magnetic system. It is seen that the total spectral weight below 140 cm^{-1} is not conserved; there is a net gain of about 6000 cm^{-2}. To clarify this point, we plot the total spectral weight of the high-frequency phonons in the inset. The high-frequency phonons are seen to suffer a net loss of 5000–10 000 cm^{-2} below T_N, which compensates for the gain of spectral weight below 140 cm^{-1} within experimental error. The change in the phonon strength in the 50–295 K range is the usual behavior from thermal contraction. Thus, we believe that the additional low-frequency modes in $Eu_{0.75}Y_{0.25}MnO_3$ are coupled to, and acquire their optical activity from, all the phonon modes.

Further evidence of coupling between the phonons and magnons is visible in the temperature dependence of the phonon frequency in Fig. 3(a). In the temperature range where phonon hardening usually saturates, we see an onset of additional hardening at T_{FE} and a smaller effect at T_N. Figure 3(b) shows the dielectric constant of $Eu_{0.75}Y_{0.25}MnO_3$. The peak at 30 K in the low-frequency curves ($e\|a$ and $e\|c$) signals the onset of the static ferroelectric (FE) moment and is related to the dynamical response of ferroelectric domains. The ir dielectric constant at ~10 cm^{-1} only reproduces a step up in ε_a, which is the signature of electric dipole activity of the additional modes in $e\|a$ polarization. Signatures of these modes were not found for $e\|c$ in either transmission spectra or $\varepsilon_c(T)$.

We now discuss the possible origin of these additional ir-active modes. We clearly observe the main signature of electromagnons (EMs)—spectral weight transfer from phonon to magnons.[4,5] However, before developing this interpretation further we consider several other possibilities.

Additional phonons. The activation of additional phonons is expected due to the structural distortions associated with the phase transitions. These can arise from the lowered crystallographic symmetry or from zone folding from a reduced Brillouin zone. In either case the strength of these modes is proportional to the square of the order parameter associated with the lattice distortions—**P**. As the lattice distortions are very small in these improper ferroelectrics, the corresponding phonons are also very weak. One example is provided by $TbMn_2O_5$ in which two phonons that are Raman active in the paraelectric phase become ir active in the FE phases.[15] Their ir strength is ~50 cm^{-2} compared with 10^4 cm^{-2} for typical ir phonons in oxides and much weaker than the features we observe in $Eu_{0.75}Y_{0.25}MnO_3$.

Ligand field levels. Low-frequency *f*-level transitions have been observed and reported in many rare earth compounds.[14] However, our observations of additional modes in $Eu_{0.75}Y_{0.25}MnO_3$ and YMn_2O_5 cannot be explained in this way. Y has no *f* levels near the Fermi level and Eu^{3+} has a ground state with J=0, and its first excited state is located around 300 cm^{-1} above the ground state.[16]

Double-well lattice model. Golovenchits *et al.*[17] interpreted a similar absorption observed in $EuMn_2O_5$ in terms of two-level states induced by magnetic inhomogeneities at domain walls. This mechanism would predict unobserved variations in strength with samples and materials. In addition, the observed crystal-structure-related polarization selection rules are incompatible with effects associated with the variable orientation of domain boundaries.

Electromagnons. The coupling of the magnons to the lattice leads to mode mixing and therefore spectral weight transfer between the electric dipole active phonons and the magnetic-dipole-active magnons.[3] The electric-dipole-activated magnon can be thought of as the Goldstone bosons of multiferroicity.[3] In general the lowest-order coupling can be written as a trilinear term in the Hamiltonian,[12] $H \sim uSS$, where u is the lattice displacement and S is the spin variable. The form of the interaction that can couple the $q=0$ phonon to one magnon is $H \sim u_0 S_{-Q} \langle S_{+Q} \rangle$, where $\langle S_{+Q} \rangle$ corresponds to the static magnetic structure.

A quantitative comparison of experiments with theory is limited by the lack of a theoretical treatment for realistic structures including both symmetric and antisymmetric exchange. Katsura *et al.*[3] have reported a theory of the EMs for the case of a spin chain with cycloidal order coupled to the lattice by Dzyaloshinskii-Moriya (DM) antisymmetric superexchange. They predict that the EM should be observed as a $e \perp \mathbf{P} \perp Q$ absorption. However, the observation is that the EM is parallel to the a axis for $Eu_{0.75}Y_{0.25}MnO_3$ as well as for $TbMnO_3$ and $GdMnO_3$, where the static polarization direction and value are different for the three compounds. Therefore the EM in the $RMnO_3$ multiferroics has a unique selection rule ($e\|a$) which is not borne out by the Katsura model. The model also predicts that the frequency of the EM should be lower than the AFMR, but, as shown above in Fig. 1, we have observed the opposite. However, the model does predict that the EM and the AFMR are separate modes, as our result also implies.

The 80 cm^{-1} feature is even more problematic within the Katsura picture. In this case the magnon at $q=Q$ is an internal mode in the unit cell and is nearly degenerate with the lowest-frequency phonon. However, since mode mixing has

generic features, it is interesting to examine the predictions of the Katsura model for this nearly degenerate case. The model can produce the large oscillator strength transfer for a large DM coupling constant but this is accompanied by a large shift, $\sim 20\ \mathrm{cm}^{-1}$, in the optical phonon. The phonon is observed to shift to higher frequencies, consistent with mode repulsion, but only $\sim 2\ \mathrm{cm}^{-1}$.

Symmetric exchange coupling should produce similar mode mixing behavior and in principle the coupling strength can be larger than is expected for DM exchange. Mostovoy[18] has shown that symmetric exchange coupling would produce a response of the form with the electromagnon parallel to **P** for simple models. While this is the observed selection rule for YMn_2O_5 and $TbMn_2O_5$ where the EM is parallel to both *b* and **P**, it is not correct for the $RMnO_3$ systems. Therefore, a full symmetry analysis of the lattice and magnetic order will be required to account for the EM selection rules. Clearly, extending the simple EM models to include more accurate depictions of the materials is an important priority.

We note that inelastic neutron scattering can provide important additional information. Data reported by Senff *et al.*[19] shows good agreement with the low-frequency ir data of $TbMnO_3$.[4] Also Lee *et al.*[20] have recently reported good agreement between the sharp EM features in YMn_2O_5 and the magnons observed in neutron scattering at $q=Q$ favoring the mode mixing scenario for that material. Mode mixing also implies the onset of magnetic dipole activity of the phonons at T_{FE}.

The trilinear coupling also allows a two-magnon decay of the phonons, by the terms $H \sim u_0 S_q S_{-q}$. The corresponding frequency-dependent phonon self-energy can produce modifications of the phonon absorption line shape related to the two-magnon ($q_1=-q_2$) density of states. As the two-magnon density of states is broad with no narrow spectral features, this process is unlikely to produce the observed relatively narrow electromagnon absorption. However, the two-magnon process is a good candidate for understanding the broad background absorption observed below as well as above T_N in the $e \| a$ polarization. The gradual decrease of this background signal with temperature (Fig. 2) above T_N suggests that it originates from magnetic fluctuations. Since there are no long-lived magnons for $T > T_N$ this background arises from the coupling of the phonon to the dynamic fluctuations of the magnetic system in the paramagnetic phase. Confirming evidence for this interpretation would be the observation of short-range magnetic order in these materials above T_N by inelastic neutron scattering.

Summarizing the above discussion we interpret our observations as follows: (1) the well-defined absorption peaks at 25 and 80 cm^{-1} arise from mode mixed phonon-magnon excitations—electromagnons, and (2) there exists colossal coupling between magnons and phonons that leads to the spectacular loss of spectral weight of the 120 cm^{-1} phonon. We assert that electromagnon excitations provide a powerful window into the physics of multiferroics and that a treatment of the magnon-phonon interaction that includes the crystal and magnetic structure may allow a better understanding of the exchange coupling mechanism responsible for the exotic magnetoelectric properties of these materials.

We thank C. Broholm, A. B. Harris, D. Khomskii, and M. Mostovoy for useful discussions. This work was supported in part by the National Science Foundation MRSEC under Grant No. DMR-0520471.

[1] S.-W. Cheong and M. Mostovoy, Nat. Mater. **6**, 13 (2007).
[2] G. Smolenskii and I. Chupis, Sov. Phys. Usp. **25**, 475 (1982).
[3] H. Katsura, A. V. Balatsky, and N. Nagaosa, Phys. Rev. Lett. **98**, 027203 (2007).
[4] A. Pimenov, A. A. Mukhin, V. Y. Ivanov, V. D. Travkin, A. M. Balbashov, and A. Loidl, Nat. Phys. **2**, 97 (2006).
[5] A. B. Sushkov, R. Valdés Aguilar, S. Park, S.-W. Cheong, and H. D. Drew, Phys. Rev. Lett. **98**, 027202 (2007).
[6] N. Hur, S. Park, P. A. Sharma, S. Guha, and S. W. Cheong, Phys. Rev. Lett. **93**, 107207 (2004).
[7] T. Kimura, G. Lawes, T. Goto, Y. Tokura, and A. P. Ramirez, Phys. Rev. B **71**, 224425 (2005).
[8] N. A. Hill and A. Filippetti, J. Magn. Magn. Mater. **242-245**, 976 (2002).
[9] J. Hemberger, F. Schrettle, A. Pimenov, P. Lunkenheimer, V. Y. Ivanov, A. A. Mukhin, A. M. Balbashov, and A. Loidl, Phys. Rev. B **75**, 035118 (2007).
[10] M. Kenzelmann, A. B. Harris, S. Jonas, C. Broholm, J. Schefer, S. B. Kim, C. L. Zhang, S.-W. Cheong, O. P. Vajk, and J. W. Lynn, Phys. Rev. Lett. **95**, 087206 (2005).
[11] P. G. Radaelli and L. C. Chapon, arXiv:cond-mat/0609087 (unpublished).
[12] A. B. Harris, arXiv:cond-mat/0610241 (unpublished).
[13] A. Pimenov, T. Rudolf, F. Mayr, A. Loidl, A. A. Mukhin, and A. M. Balbashov, Phys. Rev. B **74**, 100403(R) (2006).
[14] A. A. Mukhin, A. Y. Pronin, A. S. Prokhorov, G. V. Kozlov, V. Zelezny, and J. Petzelt, Phys. Lett. A **153**, 499 (1991).
[15] R. Valdés Aguilar, A. B. Sushkov, S. Park, S.-W. Cheong, and H. D. Drew, Phys. Rev. B **74**, 184404 (2006).
[16] M. Tovar, D. Rao, J. Barnett, S. B. Oseroff, J. D. Thompson, S.-W. Cheong, Z. Fisk, D. C. Vier, and S. Schultz, Phys. Rev. B **39**, 2661 (1989).
[17] E. I. Golovenchits, N. V. Morozov, V. A. Sanina, and L. M. Sapozhnikova, Sov. Phys. Solid State **34**, 56 (1992).
[18] M. Mostovoy (private communication).
[19] D. Senff, P. Link, K. Hradil, A. Hiess, L. P. Regnault, Y. Sidis, N. Aliouane, D. N. Argyriou, and M. Braden, Phys. Rev. Lett. **98**, 137206 (2007).
[20] S. H. Lee, J. H. Kim, J. H. Chung, Y. Qiu, M. Kenzelman, T. J. Sato, S. Park, and S.-W. Cheong, http://meetings.aps.org/link/BAPS.2007.MAR.J13.12